



Atomic and Molecular Effects on Spherically Convergent Ion Flow II: Multiple Molecular Species

G.A. Emmert and J.F. Santarius

July 2009

UWFDM-1370

Published in *Physics of Plasmas* 17, 013503 (2010).

FUSION TECHNOLOGY INSTITUTE
UNIVERSITY OF WISCONSIN
MADISON WISCONSIN

**Atomic and Molecular Effects on Spherically
Convergent Ion Flow II: Multiple Molecular
Species**

G.A. Emmert and J.F. Santarius

Fusion Technology Institute
University of Wisconsin
1500 Engineering Drive
Madison, WI 53706

<http://fti.neep.wisc.edu>

July 2009

UWFDM-1370

**Atomic and molecular effects on
spherically convergent ion flow II:
multiple molecular species**

Gilbert A. Emmert and John F. Santarius

*Fusion Technology Institute, University of Wisconsin at Madison,
1500 Engineering Drive,
Madison, Wisconsin 53706, USA
santarius@engr.wisc.edu*

ABSTRACT

A theoretical model for the effect of molecular interactions on the flow of molecular ions in spherically convergent geometry where the inner grid (cathode) is at a large negative potential and the outer grid (anode) is grounded has been developed. The model assumes a weakly ionized deuterium plasma composed of D^+ , D_2^+ , and D_3^+ ions which interact with the dominant background gas (D_2). The interactions included are charge exchange, ionization, and dissociative processes. The formalism developed includes the bouncing motion of the ions in the electrostatic well and sums over all generations of subsequent ions produced by atomic and molecular processes. This leads to a set of two coupled Volterra integral equations which are solved numerically. From the solution of the Volterra equations one can obtain quantities of interest, such as the energy spectra of the ions and fast neutral atoms and molecules, and the fusion reaction rate. To provide an experimental test, the model is applied to inertial electrostatic devices and the calculated neutron production rate is compared with previously reported measurements for one University of Wisconsin inertial-electrostatic confinement (IEC) device [D. C. Donovan, D. R. Boris, G. L. Kulcinski, and J. F. Santarius, *Fusion Sci. Technol.* **56**, 507 (2009)]. The results show general agreement with the experimental results, but significant differences remain to be resolved.

I. INTRODUCTION

In a companion paper,¹ a model for spherically convergent ion flow was developed; the model assumed the ions and the background gas were atomic, such as helium ions interacting with helium gas. In this paper, we extend this model to include deuterium molecular ions (D^+ , D_2^+ , and D_3^+). This work is particularly relevant to inertial electrostatic confinement (IEC) devices using deuterium as the working gas. The geometric configuration consists of two concentric spherical, nearly transparent electrodes with the outer electrode grounded and the inner electrode at a large negative potential (see Fig. 1). Ions are created in the region outside the outer electrode and are accelerated towards the center by the electric field. For moderate pressure operation (a few mTorr), the ions undergo charge exchange and dissociative processes, while

inducing ionization of the background D_2 gas, on their way to the center; the mean free path for these processes is comparable with the size of the device. These atomic and molecular processes degrade the energy of the ions, while increasing the ion flux; they also produce energetic neutral atoms and molecules which stream throughout the vacuum chamber.

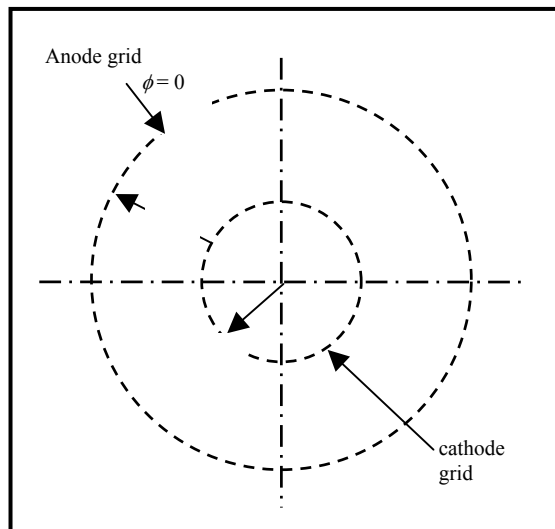


Figure 1. Schematic showing the geometry. The anode grid is grounded, the cathode grid is at a large negative potential. Ions enter from the source region outside the anode grid and are accelerated towards the center by the electric field.

II. MOLECULAR REACTIONS INCLUDED

The plasma created in the source region is assumed to be a mixture of D^+ , D_2^+ , and D_3^+ ions. The ion densities are assumed to be sufficiently low that ion interactions with the background gas dominate over ion-ion interactions. The ions from the source region enter the intergrid region, collide with the background D_2 gas, and dissociate to form a variety of fast and slow products (D_2^+ , D^+ , D_2 , and D). The interactions between D^+ , D_2^+ , and D_3^+ with the background gas that we include in this analysis are shown in Table I.

The cross sections are defined in Table I; we use the s superscript to denote the production of slow ions, the f superscript to denote the production of fast ions, and the d superscript to denote the total destruction cross section. We also denote the species of the parent ion by the first subscript and the daughter ion by the second subscript. These cross sections are, for the most part, available in the literature². Note that some of these processes are sums over different reaction channels that lead to the same end products. Since we are interested in the energy range from thermal energies to about 300 keV, which is appropriate to IEC devices, interpolations and extrapolations have been used to fill in gaps in the published cross section data. The cross section data are mostly for hydrogen ions (H^+ , H_2^+ , and H_3^+) interacting with H_2 gas; we use these for deuterium interactions at the same energy per amu of the incident particle. There are also cross-sections for forming fast neutral atoms and molecules (see Table II). We

don't need these for the ion dynamics, but will need them to compute the fusion reaction rate from fast neutral atoms and molecules striking the background gas. These are also available in the literature.²

Table 1. Interactions Included in the Model.

Reaction	Process	Cross section
$D^+ + D_2 \rightarrow \text{various products}$	Total destruction of D^+	σ^d_1
$D^+ + D_2 \rightarrow D^+ + \dots$	Stationary D^+ production	σ^s_{11}
$D^+ + D_2 \rightarrow D_2^+ + \dots$	Stationary D_2^+ production	σ^s_{12}
$D_2^+ + D_2 \rightarrow \text{various products}$	Total destruction of D_2^+	σ^d_2
$D_2^+ + D_2 \rightarrow D^+ + \dots$	Fast D^+ production	σ^f_{21}
$D_2^+ + D_2 \rightarrow D^+ + \dots$	Stationary D^+ production	σ^s_{21}
$D_2^+ + D_2 \rightarrow D_2 + D_2^+$	Stationary D_2^+ production	σ^s_{22}
$D_3^+ + D_2 \rightarrow \text{various products}$	Total destruction of D_3^+	σ^d_3
$D_3^+ + D_2 \rightarrow D^+ + \dots$	Fast D^+ production	σ^f_{31}
$D_3^+ + D_2 \rightarrow D_2^+ + \dots$	Fast D_2^+ production	σ^f_{32}
$D_3^+ + D_2 \rightarrow D^+ + \dots$	Stationary D^+ production	σ^s_{31}
$D_3^+ + D_2 \rightarrow D_2^+ + \dots$	Stationary D_2^+ production	σ^s_{32}

Unfortunately, the cross-sections for producing slow D_2^+ and D^+ ions from D_3^+ striking D_2 , and for producing slow D^+ ions from D_2^+ striking D_2 are not available. To fill in the missing data, we use a reaction channel model for the interaction. In the case of D_3^+ colliding with D_2 , we assume the relevant reaction channels are charge exchange, dissociation, and dissociative charge transfer. We determine the cross sections for each channel by fitting to the known cross sections for forming fast ions and neutral atoms or molecules; we then compare the calculated

destruction cross section with the measured value to determine the “goodness” of the model. With this choice, we can then determine the total cross section for forming slow reaction product ions. The result is that

$$\sigma_{31}^s + \sigma_{32}^s = \sigma_3^d - \sigma_{31}^f - \sigma_{32}^f, \quad (1)$$

which is what we expect from charge conservation. For D_2^+ , we assume the relevant reaction channels are charge exchange, dissociation, dissociative charge exchange and dissociative ionization. Using measured cross sections for charge exchange and dissociation, we can determine the other reaction channel cross sections by fitting to the measured cross sections for forming fast D^+ ions and D atoms. The result is that the cross section for forming slow D^+ should satisfy

$$\sigma_{21}^s = \frac{1}{2}(\sigma_{21}^{fn} + \sigma_{21}^f) - \sigma_2^d. \quad (2)$$

Table 2. Notation for cross sections for forming fast neutral atoms and molecules.

Cross section	Process
σ_{11}^{fn}	Production of fast D from D^+ incident on D_2
σ_{21}^{fn}	Production of fast D from D_2^+ incident on D_2
σ_{22}^{fn}	Production of fast D_2 from D_2^+ incident on D_2
σ_{31}^{fn}	Production of fast D from D_3^+ incident on D_2
σ_{32}^{fn}	Production of fast D_2 from D_3^+ incident on D_2

In Eq. (1) we only get a limit on the sum of σ_{31}^s and σ_{32}^s ; lacking further information, we assume the slow ions formed are D^+ . With these assumptions we get specific values for the missing cross sections. The cross sections used in this analysis are shown in Fig. 2 as a function of the projectile energy.

Since the reactions listed in Table I normally do not involve significant momentum transfer from one molecule (or ion) to the other, we will assume the daughter products have the same speed as the parent. Consequently the daughter ions have finite speed at birth if they were created by dissociation of an energetic parent ion. If the daughter ion was created by charge transfer to the background D_2 molecule, or ionization (including dissociative ionization) of the background D_2 molecule, then the daughter ion will be assumed to be born stationary.

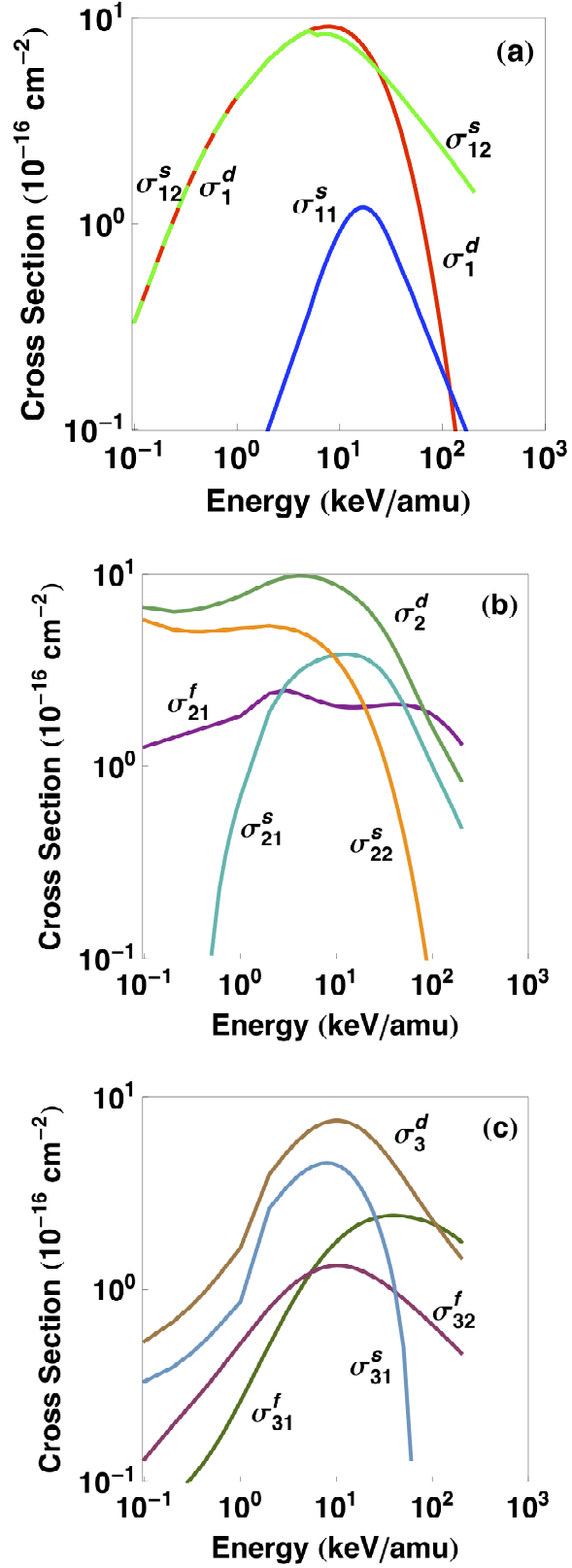


Figure 2. Cross sections for forming fast and slow ions: (a) D^+ interacting with D_2 , (b) D_2^+ interacting with D_2 , (c) D_3^+ interacting with D_2 .

III. INTEGRAL EQUATIONS FOR ION TRANSPORT IN THE IEC

The integral equations for molecular ion transport are straightforward generalizations of those developed for atomic ions in the companion paper¹. We use the terminology that was developed there; we define class I ions as those ions that enter the intergrid region from the source region and class II ions as those ions that are born within the intergrid and cathode regions. There are three types of class I ions: D^+ , D_2^+ , and D_3^+ . Class I D_3^+ ions from the source region enter the intergrid region and react with D_2 to produce D_2^+ and D^+ ions, both fast and stationary. Class I D_2^+ ions react with D_2 to produce stationary D_2^+ and both fast and stationary D^+ ions. Class I D^+ ions react with D_2 to produce stationary D^+ and D_2^+ ions. Thus we get an internal source of both fast and stationary D^+ and D_2^+ ions in the cathode and intergrid region; these are called class II ions. Stationary D^+ and D_2^+ ions are accelerated by the electric field to become energetic; they can then interact with the background gas to produce subsequent generations of class II D^+ and D_2^+ ions in the intergrid and cathode regions. This leads to two coupled integral equations, one for each species of class II ions.

To develop the integral transport equations we start with the class I ions entering from the source region. We define Γ_0 to be the ion flux leaving the anode and heading inward, and h_i to be the fraction in the i th species, where $i=1$ denotes D^+ , $i=2$ denotes D_2^+ and $i=3$ denotes D_3^+ . We define the attenuation function for the i th species,

$$f_i(r) = \exp \left\{ \int_r^b n_g \sigma_i^d [E(r')] dr' \right\}, \quad (3)$$

where

$$E(r') = E_0 - q\phi(r') \quad (4)$$

is the kinetic energy of a class I ion at the radius r' . The (non-directed) flux of the i th species class I ions at the radius r is

$$\Gamma_i(r) = \frac{b^2 h_i \Gamma_0}{r^2} \left[f_i(r) + T_c^2 \frac{f_i^{cp}}{f_i(r)} \right]. \quad (5)$$

where we have introduced the complete pass attenuation function,

$$f_i^{cp} = f_i^2(0). \quad (6)$$

The first term in the square bracket in Eq. (5) is the contribution from inward traveling ions and the second term is the contribution from outward traveling ions. From the flux of class I ions of species i at radius r we can calculate the source term for the creation of first generation class II ions at the radius r ,

$$A_i^s(r) = n_g \sum_{j=1}^3 \Gamma_j(r) \sigma_{ji}^s. \quad (7)$$

Substituting from Eq. (5) for the flux, we get the source term for first generation class II ions,

$$A_i^s(r) = \frac{b^2}{r^2} n_g \Gamma_0 \sum_{j=1}^3 h_j \left[f_j(r) + T_c^2 \frac{f_j^{cp}}{f_j(r)} \right] \sigma_{ji}^s, \quad i=1,2, \quad (8)$$

due to the class I ions crossing the anode and heading inward.

So far the analysis considers only daughter ions that are born cold. However, daughter ions created by dissociation of the fast parent ion have the speed of the parent, so they can't be included in the $A^s(r)$ as defined so far. To include the ions born with finite speed, we shift them to their turning point, where they are stationary, and put them into the source of next generation ions at that location. For those ions born with positive radial velocity, this shifts the starting point

of their track forward; for ions born with negative radial velocity, this shifts the starting point of their track backwards. To lowest order in the asymmetry between the inward and outward radial velocities, these shifts cancel.

Consider an ion which was born at radius r' with kinetic energy E_0 (we include E_0 so that we can treat parent ions of class I as well as class II in the same equation). Assume the parent reaches the radius r'' where it undergoes dissociation to create a daughter ion. The parent ion has kinetic energy

$$E_p(r'') = q[\phi(r') - \phi(r'')] + E_0. \quad (9)$$

Define m to be the number of nuclei in the parent ion and n to be the number of nuclei in the resulting daughter ion. Since the daughter has the same velocity as the parent, its kinetic energy at birth is

$$E_d(r'') = \frac{n}{m} E_p(r''). \quad (10)$$

The daughter will have its turning point at the radius r , where

$$E_d(r'') + q\phi(r'') = q\phi(r). \quad (11)$$

Substituting from Eqs. (9) and (10) and solving for the potential at the birth point of the daughter, we get

$$\phi(r'') = \frac{m\phi(r) - n\phi(r') - n\frac{E_0}{q}}{m - n}. \quad (12)$$

From Eq. (12) we can determine the daughter birth point, r'' , for a given turning point, r , and origin of the parent ion, r' . For class I parent ions, $r' = b$ (the anode radius) and E_0 is given by the input value; for class II parent ions, $r' =$ their birth point and $E_0 = 0$.

Class I D_2^+ ions entering from the anode and interacting with the background gas will create slow and fast D^+ ions and slow D_2^+ ions. The slow D^+ and D_2^+ ions have been included in the analysis above. We now consider the fast D^+ ions created by the D_2^+ ions. The fast ions born at a radius r'' will have their turning points at a radius r . The number of fast ions created per unit time in a shell of radius r'' and thickness dr'' is $n_g \Gamma_2(r'') \sigma_{21}^f [E(r'')] 4\pi r''^2 dr''$, where the non-directed flux Γ_2 is given by Eq. (5). We now move these ions from the shell at radius r'' to a shell of thickness dr at radius r ; conserving the number of ions yields the resulting ‘‘cold’’ ion source density at radius r ,

$$A_1^{f1}(r) (4\pi r^2 dr) = n_g \Gamma(r'') \sigma_{21}^f [E(r'')] 4\pi r''^2 dr''. \quad (13)$$

Substituting for $\Gamma(r'')$, this becomes

$$A_1^{f1}(r) = n_g \frac{b^2}{r^2} h_2 \Gamma_0 \left[f_2(r'') + T_c^2 \frac{f_2^{cp}}{f_2(r'')} \right] \sigma_{21}^f [E(r'')] \frac{dr''}{dr}. \quad (14)$$

The two shell thicknesses, dr'' and dr , are not independent, but have to be related by Eq. (12). Since we are moving ions to their turning points, those on the inner edge of the shell at r'' map to the inner edge of the shell at radius r , and those on the outer edge at radius r'' map to the outer edge at radius r . Differentiating Eq. (12) with respect to r , we get

$$\frac{dr''}{dr} = \frac{mE_f(r)}{(m - n)E_f(r'')}, \quad (15)$$

where $E_f(r)$ is the electric field at the radius r . Using Eq. (15), the equivalent source term at radius r is

$$A_1^{f1}(r) = n_g \frac{b^2}{r^2} h_2 \Gamma_0 \left[f_2(r'') + T_c^2 \frac{f_2^{cp}}{f_2(r'')} \right] \sigma_{21}^f [E(r'')] \frac{mE_f(r)}{(m-n)E_f(r'')}. \quad (16)$$

Equation (16) incorporates the fast daughter ions born in the intergrid region, but does not include the fast ions born in the cathode region where the potential is constant. For a given parent ion, all the fast daughter ions born in the cathode region have the same turning point. The number of fast daughter ions created per unit volume per second in the cathode region by class I D_2^+ parent ions is

$$\frac{b^2}{r''^2} h_2 \Gamma_0 T_c \left[f_2(r'') + \frac{f_2^{cp}}{f_2(r'')} \right] n_g \sigma_{21}^f [E(r'')]. \quad (17)$$

We integrate this over the cathode region to get the number created per second,

$$4 \pi b^2 h_2 n_g \Gamma_0 T_c \int_0^a \left[f_2(r'') + \frac{f_2^{cp}}{f_2(r'')} \right] \sigma_{21}^f [E(r'')] dr''. \quad (18)$$

These ions are to be placed at their turning point, r_{imn} , which is gotten by solving Eq. (12);

$$\phi(r_{imn}) = \frac{m-n}{m} \phi_c + \frac{n}{m} \phi(r') + \frac{nE_0}{mq}, \quad (19)$$

where ϕ_c is the potential in the cathode region. [In using Eq. (19), we put $\phi(r') = 0$, $E_0 \neq 0$ for class I ions, and $\phi(r') \neq 0$, $E_0 = 0$ for class II ions.] Consequently, this contribution to the source function $A(r)$ is given by

$$A_1^{f2}(r) = \frac{b^2}{r^2} h_2 n_g \Gamma_0 T_c \int_0^a \left[f_2(r'') + \frac{f_2^{cp}}{f_2(r'')} \right] \sigma_{21}^f [E(r'')] dr'' \delta(r - r_{i21}), \quad (20)$$

where we have introduced the Dirac delta function to ensure that the ions are placed only in the shell at radius r_{imn} .

In the cathode region, the energy $E(r'')$ is constant and the attenuation function, $f_i(r'')$, is a simple exponential function of r'' ,

$$f_i(r'') = f_i(0) \exp(\alpha_i r'') = \sqrt{f_2^{cp}} \exp(\alpha_i r''), \quad (21)$$

where $\alpha_i = n_g \sigma_i^d [E(a)]$, so the integral in Eq. (20) can be done analytically;

$$\int_0^a \left[f_i(r'') + \frac{f_2^{cp}}{f_i(r'')} \right] \sigma_{21}^f [E(r'')] dr'' = \sigma_{ij}^f [E(a)] \frac{\sqrt{f_2^{cp}}}{\alpha_i} [\exp(\alpha_i a) - \exp(-\alpha_i a)]. \quad (22)$$

The generalization of the integral equation analysis to include the fast ions is now clear. Adding the slow, $A_1^s(r)$, and two fast, $A_1^{f1}(r)$ and $A_1^{f2}(r)$, daughter ion contributions from both class I D_2^+ and D_3^+ ions, the total source term for class II D^+ ions becomes

$$\begin{aligned}
A_1(r) = & \frac{b^2}{r^2} n_g \Gamma_0 \left\{ h_1 \left[f_1(r) + T_c^2 \frac{f_1^{cp}}{f_1(r)} \right] \sigma_{11}^s [E(r)] + h_2 \left[f_2(r) + T_c^2 \frac{f_2^{cp}}{f_2(r)} \right] \sigma_{21}^s [E(r)] \right. \\
& + h_3 \left[f_3(r) + T_c^2 \frac{f_3^{cp}}{f_3(r)} \right] \sigma_{31}^s [E(r)] + h_2 \left[f_2(r_{21}'') + T_c^2 \frac{f_2^{cp}}{f_2(r_{21}'')} \right] \sigma_{21}^f [E(r_{21}'')] \frac{2E_f(r)}{E_f(r_{21}'')} \\
& + h_3 \left[f_3(r_{31}'') + T_c^2 \frac{f_3^{cp}}{f_3(r_{31}'')} \right] \sigma_{31}^f [E(r_{31}'')] \frac{3E_f(r)}{2E_f(r_{31}'')} + \\
& + h_2 T_c \int_0^a \left[f_2(r'') + \frac{f_2^{cp}}{f_2(r'')} \right] \sigma_{21}^f [E(r'')] dr'' \delta(r - r_{t21}) \\
& \left. + h_3 T_c \int_0^a \left[f_3(r'') + \frac{f_3^{cp}}{f_3(r'')} \right] \sigma_{31}^f [E(r'')] dr'' \delta(r - r_{t31}) \right\}. \tag{23}
\end{aligned}$$

The first three terms on the right-hand side give the contribution from slow D^+ ion production, and the next two terms give the contribution from fast D^+ ion production at the radius r_{21}'' or r_{31}'' (in the intergrid region), where they have a total energy that carries them to the turning point at r . The last two terms give the contribution from fast D^+ ions born in the cathode region; they have turning points at radii r_{t21} and r_{t31} . We use Eq. (22) to evaluate the integral in the last two terms.

The source term for class II D_2^+ ions becomes, with terms analogous to those in Eq. (23),

$$\begin{aligned}
A_2(r) = & \frac{b^2}{r^2} n_g \Gamma_0 \left\{ h_1 \left[f_1(r) + T_c^2 \frac{f_1^{cp}}{f_1(r)} \right] \sigma_{12}^s [E(r)] \right. \\
& + h_2 \left[f_2(r) + T_c^2 \frac{f_2^{cp}}{f_2(r)} \right] \sigma_{22}^s [E(r)] + h_3 \left[f_3(r) + T_c^2 \frac{f_3^{cp}}{f_3(r)} \right] \sigma_{32}^s [E(r)] \\
& + h_3 \left[f_3(r_{32}'') + T_c^2 \frac{f_3^{cp}}{f_3(r_{32}'')} \right] \sigma_{32}^f [E(r_{32}'')] \frac{3E_f(r)}{E_f(r_{31}'')} \\
& \left. + h_3 T_c \int_0^a \left[f_3(r'') + \frac{f_3^{cp}}{f_3(r'')} \right] \sigma_{32}^f [E(r'')] dr'' \delta(r - r_{t32}) \right\}. \tag{24}
\end{aligned}$$

For subsequent generations of class II ions, we follow the same approach used in the atomic model.¹ We now have two species of class II ions, so we introduce S_1 as the source term for D^+ ions, and S_2 as the source term for D_2^+ ions. Energetic D^+ ions can produce cold D_2^+ ions by ionization of the D_2 gas, and energetic D_2^+ ions can produce cold D^+ ions by dissociative ionization of the D_2 gas. Consequently, we get two coupled integral equations for the cold D^+ and D_2^+ source functions, respectively,

$$S_1(r) = A_1(r) + \int_r^b K_{11}(r, r') S_1(r') dr' + \int_r^b K_{12}(r, r') S_2(r') dr', \tag{25}$$

$$S_2(r) = A_2(r) + \int_r^b K_{21}(r, r') S_1(r') dr' + \int_r^b K_{22}(r, r') S_2(r') dr'. \tag{26}$$

To obtain the kernels, K_{ij} , we follow the same procedure as in companion paper¹ of this paper. However, now there are kernel cross terms, K_{12} and K_{21} , since D^+ ions can produce D_2^+

ions, and vice versa. It is also convenient to split the kernels into the slow and fast daughter ion contributions,

$$K_{ij}(r, r') = K_{ij}^s(r, r') + K_{ij}^f(r, r'). \quad (27)$$

By straightforward generalization of the procedure used in the companion paper,¹ the slow daughter ion contributions to the kernels are

$$K_{ij}^s(r, r') = n_g \sigma_{ji}^s [E(r, r')] \left(\frac{r'^2}{r^2} \right) \left[g_i(r, r') + \frac{T_c^2 g_i^{cp}(r')}{g_i(r, r')} \right] \frac{1}{1 - T_c^2 g_i^{cp}(r')}. \quad (28)$$

where we have introduced the attenuation function,

$$g_i(r, r') = \exp \left\{ -n_g \int_r^{r'} \sigma_i^d [E(r'', r')] dr'' \right\} \quad (29)$$

which measures the probability of an ion born at r' reaching the radius r . We have also introduced the complete pass probability,

$$g_i^{cp}(r') = [g_i(0, r')]^2, \quad (30)$$

which is the probability of an ion born at radius r' to reach the origin and return to the radius r' . The cross-sections are a function of the energy

$$E(r, r') = q[\phi(r') - \phi(r)], \quad (31)$$

which is the energy of an ion at radius r that was born at radius r' .

The fast contributions, K_{ij}^f , are zero, except for $i=1, j=2$, which is caused by class II D_2^+ ions interacting with the background gas and dissociating to produce fast class II D^+ ions. We use the same procedure as for daughter ions produced by class I ions; we shift them from the birth point to their turning point. The resulting kernel is

$$\begin{aligned} K_{12}^f(r, r') = & n_g \sigma_{21}^f [E(r_{21}^'', r')] \left(\frac{r'^2}{r^2} \right) \left[g_2(r_{21}^'', r') + \frac{T_c^2 g_2^{cp}(r')}{g_2(r_{21}^'', r')} \right] \frac{1}{1 - T_c^2 g_2^{cp}(r')} \frac{2E_f(r)}{E_f(r_{21}^'')} \\ & + n_g \left(\frac{r'^2}{r^2} \right) T_c \int_0^d \left[g_2(r'', r') + \frac{g_2^{cp}(r')}{g_2(r'', r')} \right] \sigma_{21}^f [E(r'', r')] dr'' \frac{1}{1 - T_c^2 g_2^{cp}(r')} \delta[r - r_t(r')]. \end{aligned} \quad (32)$$

The first term on the right side of Eq. (32) is the contribution of fast D^+ ions born at radius $r_{21}^''$ in the intergrid region from parent D_2^+ ions born at radius r' ; the daughter ions have turning points at radius r . For a given r and r' , the birth point is calculated using Eq. (12) with $m=2, n=1$, and $E_0=0$. The second term on the right side of Eq. (32) is the contribution of fast D^+ ions born at radius $r_{21}^''$ in the cathode region; these ions all have their turning point at the radius $r_t(r')$, where r' is the parent's birth point. The turning point $r_t(r')$ is the solution of Eq. (12) with $m=2, n=1$, and $E_0=0$.

In the cathode region, the g_2 attenuation function varies exponentially,

$$g_2(r'', r') = g_2(0, r') \exp(\alpha_2 r'') = \sqrt{g_2^{cp}(r')} \exp(\alpha_2 r''), \quad (33)$$

where $\alpha_2 = n_g \sigma_2^d(E(a, r'))$. In addition, the energy $E(r'', r')$ is independent of r'' in the cathode region. This allows the integral involving the g_2 function to be done analytically;

$$\int_0^d \left[g_2(r'', r') + \frac{g_2^{cp}(r')}{g_2(r'', r')} \right] \sigma_{21}^f [E(r'', r')] dr'' = \sigma_{21}^f [E(a, r')] \frac{\sqrt{g_2^{cp}(r')}}{\alpha_2} [\exp(\alpha_2 a) - \exp(-\alpha_2 a)]. \quad (34)$$

The two coupled Volterra equations [Eq. (25) and (26)] are solved numerically to obtain the source

functions $S_1(r)$ and $S_2(r)$; the numerical method is described in Appendix A. Detailed information about the ion energy spectra, etc., can then be calculated from these source functions.

IV. NEUTRON PRODUCTION

Neutron production from $D(d,n)^3\text{He}$ reactions is a convenient diagnostic tool, as well as one of the applications of inertial electrostatic confinement devices. In this section we use the integral transport equation to determine the total neutron production rate. We consider energetic ions and fast neutral atoms or molecules fusing with the background gas, but do not include fusion reactions due to ion-ion or ion-fast neutral atom collisions.

A. Ion – neutral gas fusion

We start with the class I ions coming from the anode. The non-directed ion flux of type i ions at a point r in the intergrid and cathode regions is given by Eq. (5). The rate of neutron production from these ions colliding with the background gas is

$$\dot{N}_{1i} = i(2n_g) \int_0^b \sigma_f \left(\frac{E}{i} \right) \Gamma_i(r) 4\pi r^2 dr, \quad (35)$$

In Eq. (35), the factor i comes from one nucleus per D^+ ion ($i = 1$), two nuclei per D_2^+ ion ($i = 2$), and three nuclei per D_3^+ ion ($i = 3$). The factor 2 comes from two nuclei per D_2 molecule in the background gas; the $D(d,n)\text{He}^3$ fusion cross-section, σ_f , is evaluated at the energy per nucleus, $E(r)/i$, where $E(r)$ is given by Eq. (4). Substituting from Eq. (5), this becomes

$$\dot{N}_{1i} = i8\pi n_g b^2 h_i \Gamma_0 \left\{ \int_a^b \sigma_f \left(\frac{E}{i} \right) \left[f_i(r) + T_c^2 \frac{f_i^{cp}}{f_i(r)} \right] dr + T_c \int_0^a \sigma_f \left(\frac{E}{i} \right) \left[f_i(r) + \frac{f_i^{cp}}{f_i(r)} \right] dr \right\}, \quad (36)$$

where we have written the cathode and intergrid region contributions to the integral separately. The integral over the cathode region can be done analytically,

$$\int_0^a \sigma_f \left(\frac{E}{i} \right) \left[f_i(r) + \frac{f_i^{cp}}{f_i(r)} \right] dr = \sigma_f \left[\frac{E(0)}{i} \right] \frac{\sqrt{f_i^{cp}}}{\alpha_i} [\exp(\alpha_i a) - \exp(-\alpha_i a)], \quad (37)$$

where $\alpha_i = n_g \sigma_i^d [E(a)]$.

Next we consider class II ions of type i born in a shell of thickness dr' at a radius r' ; their flux at a radius r is

$$d\Gamma_i(r) = \left(\frac{r'}{r} \right)^2 S_i(r') \left[g_i(r, r') + T_c^2 \frac{g_i^{cp}(r')}{g_i(r, r')} \right] \frac{1}{1 - T_c^2 g_i^{cp}(r')} dr'. \quad (38)$$

Integrating over both r' and r gives this contribution to the neutron production;

$$\dot{N}_{2i} = i(2n_g) 4\pi \int_a^b \int_r^b \sigma_f \left[\frac{E(r, r')}{i} \right] S_i(r') \left[g_i(r, r') + T_c^2 \frac{g_i^{cp}(r')}{g_i(r, r')} \right] \frac{r'^2}{1 - T_c^2 g_i^{cp}(r')} dr' dr, \quad (39)$$

where the energy of an ion at r that was born at r' is given by Eq. (31), the index i in Eq. (39) takes the values $i = 1$ and $i = 2$.

The contribution from the cathode region is similar, except that the class II ions were born in the intergrid region. This contribution to the neutron production is

$$\dot{N}_{3i} = i(2n_g) 4\pi T_c \int_0^a \int_a^b \sigma_f \left[\frac{E(r, r')}{i} \right] S_i(r') \left[g_i(r, r') + \frac{g_i^{cp}(r')}{g_i(r, r')} \right] \frac{r'^2}{1 - T_c^2 g_i^{cp}(r')} dr' dr. \quad (40)$$

Note that the integration over r is from 0 to a and the integration over r' is from a to b . We can

reverse the order of the integrations and do the r integration analytically because, for $0 \leq r \leq a$, $E(r, r') = E(a, r')$. We get

$$\int_0^a \left[g_i(r, r') + \frac{g_i^{cp}(r')}{g_i(r, r')} \right] dr = \frac{\sqrt{g_i^{cp}(r')}}{\alpha_i} [\exp(\alpha_i a) - \exp(-\alpha_i a)], \quad (41)$$

where $\alpha_i = n_g \sigma_i^d [E(a, r')]$. The neutron production rate becomes

$$\dot{N}_{3i} = i 8\pi T_c \int_a^b S_i(r') \frac{\sigma_f \left[\frac{E(a, r')}{i} \right]}{\sigma_{id} [E(a, r')]} \sqrt{g_i^{cp}(r')} \frac{[\exp(\alpha_i a) - \exp(-\alpha_i a)]}{1 - T_c^2 g_i^{cp}(r')} r'^2 dr' \quad (42)$$

The total rate of neutron production from ion – background gas interactions is then

$$\dot{N}_{ion} = \sum_{i=1}^3 \dot{N}_{1i} + \sum_{i=1}^2 \dot{N}_{2i} + \sum_{i=1}^2 \dot{N}_{3i}. \quad (43)$$

B. Fusion from fast neutral atoms and molecules striking background gas

Fast deuterium atoms and molecules can be produced in the interaction of D^+ , D_2^+ , and D_3^+ ions with the background D_2 gas. We introduce the notation shown in Table II. Note that some of these cross sections are sums over several different reaction channels. For example, σ_{21}^{fn} is the sum of the cross sections for $D_2^+ + D_2 \rightarrow (D^+ + D)_{fast} + \text{slow products}$ and $D_2^+ + D_2 \rightarrow (D + D)_{fast} + \text{slow products}$. The cross sections σ_{11}^{fn} and σ_{22}^{fn} are for pure charge exchange. Cross section data for the hydrogen counterpart to these reactions are available;² we use this data for deuterium interactions at the same energy per unit mass, since the cross sections should be essentially independent of the isotope involved.

For the purposes of calculating the rate of neutron production by fusion reactions, it is immaterial whether the fast nuclei are in the form of atoms or molecules. Hence it is convenient to consider them as atoms with a speed equal to the speed of their parent ion. We introduce the short-hand notation

$$\sigma_i^n = \begin{cases} \sigma_{11}^{fn} & i = 1 \\ \sigma_{21}^{fn} + 2\sigma_{22}^{fn} & i = 2 \\ \sigma_{31}^{fn} + 2\sigma_{32}^{fn} & i = 3 \end{cases} \quad (44)$$

It is also convenient to use the term “charge exchange” as short-hand terminology to mean any process producing fast neutral atoms or molecules.

Consider a flux of class I ions of type i at energy E_0 leaving the anode surface of radius b and heading inward. The ions are accelerated by the potential and therefore have kinetic energy E , given by Eq. (4), at the radius r' . The neutral atoms produced at r' from these ions have the same speed, and therefore the energy $E(r')/i$. Inward traveling ions will produce inward traveling fast neutrals, which pass through the cathode and become outward traveling neutrals. Outward traveling ions at r' produce additional outward traveling fast neutrals, but only for $r > r'$.

We start with the inward traveling ions of type i and consider a shell of radius r' and thickness dr' , where inward traveling ions with energy E produce fast neutrals by charge exchange. The number of fast neutrals created per unit time per unit volume at radius r' is

$$S_n(r') = n_g \sigma_i^n [E(r')] \Gamma_i^{in}(r'), \quad (45)$$

where the inward ion flux is

$$\Gamma_i^{in}(r') = \frac{b^2}{r'^2} h_i \Gamma_0 f_i(r'). \quad (46)$$

This volume source of fast neutrals will produce a flux of fast neutrals of energy E/i at a radius r , where $r < r'$. The fast atom flux at r is

$$d\Gamma_n(r) = \left(\frac{r'}{r}\right)^2 S_n(r') dr' = \left(\frac{b}{r}\right)^2 n_g \sigma_i^n [E(r')] h_i \Gamma_0 f_i(r') dr'. \quad (47)$$

The number of neutrons generated per second by D-D fusion in the shell at radius r with thickness dr is

$$d^2 \dot{N} = 2n_g d\Gamma_n(r) \sigma_f \left[\frac{E(r')}{i} \right] 4\pi r^2 dr, \quad (48)$$

where σ_f is the appropriate fusion cross-section. We introduce the shorthand notation

$$\sigma_i^n(r') = \sigma_i^n [E(r')], \quad \sigma_f(r') = \sigma_f \left[\frac{E(r')}{i} \right]. \quad (49)$$

and insert from Eq. (47) for $d\Gamma_n$ to get

$$d^2 \dot{N} = 8\pi b^2 n_g^2 \sigma_{in}^n(r') \sigma_f(r') h_i \Gamma_0 f_i(r') dr' dr. \quad (50)$$

Next we integrate over r to get the total neutron production from the neutrals produced by charge exchange in the shell dr' . Now

$$\int dr = T_c \int_0^a dr + \int_a^{r'} dr. \quad (51)$$

The factor T_c accounts for the reduction of the atom flux in the cathode region because of the grid transparency. The second integration stops at r' because the fast neutrals are inward traveling and don't reach $r > r'$. Once the inward traveling fast neutrals reach the origin, they become outward traveling fast neutrals and generate fusion events all the way to the wall. Thus we get an additional contribution

$$\int dr = T_c \int_0^a dr + T_c^2 \int_a^b dr + T_c^2 T_a \int_b^c dr, \quad (52)$$

where T_a is the transparency of the anode grid, and c is the equivalent spherical radius of the vacuum chamber. The first term in Eq. (52) is the outward traveling neutrals inside the cathode, the second term is the intergrid region (the neutrals passed through the cathode grid twice to get there) and the third term is the contribution from the region between the anode (transparency T_a) and the vacuum wall. Putting all these together and evaluating the integrals, we get

$$\int dr = r' + A, \quad (53)$$

$$\text{where } A = 2T_c a - a + T_c^2(b - a) + T_c^2 T_a(c - b). \quad (54)$$

Consequently, the integration of Eq. (49) over r yields

$$d\dot{N} = 8\pi b^2 n_g^2 \sigma_i^n(r') \sigma_f(r') h_i \Gamma_0 f_i(r') (r' + A) dr'. \quad (55)$$

We now integrate over the radius r' to cover the shells that produce the charge exchange neutrals from the inward traveling ions. We get

$$\dot{N} = 8\pi b^2 n_g^2 h_i \Gamma_0 \int_a^b \sigma_i^n(r') \sigma_f(r') f_i(r') (r' + A) dr'. \quad (56)$$

This gives the neutrons generated by fast nuclei produced from inward traveling class I ions as they traverse the intergrid region.

We also have to consider outward traveling class I ions in the intergrid region. Following the same procedure, the number of neutrons generated per second in the shell dr is now

$$d^2\dot{N} = 8\pi b^2 n_g^2 \sigma_i^n(r') \sigma_f(r') h_i \Gamma_0 T_c^2 \left[\frac{f_i^{cp}}{f_i(r')} \right] dr' dr. \quad (57)$$

Integrating over dr gives

$$\int dr = \int_{r'}^b dr + T_a \int_b^c dr = (b - r') + T_a(c - b). \quad (58)$$

We integrate over dr' to get

$$\dot{N} = 8\pi b^2 n_g^2 h_i \Gamma_0 T_c^2 \int_a^b \sigma_i^n(r') \sigma_f(r') \left[\frac{f_i^{cp}}{f_i(r')} \right] (B - r') dr', \quad (59)$$

$$\text{where } B = b(1 - T_a) + T_a c. \quad (60)$$

This contribution is to be added to the contribution in Eq. (56). We combine these to get the following expression

$$\dot{N} = 8\pi b^2 n_g^2 h_i \Gamma_0 \int_a^b \sigma_i^n(r') \sigma_f(r') \left\{ (r' + A) f_i(r') + T_c^2 (B - r') \left[\frac{f_i^{cp}}{f_i(r')} \right] \right\} dr'. \quad (61)$$

We also have to consider charge exchange of class I ions as they traverse the cathode region. Since our model for the potential assumes a constant potential inside the cathode, the ions have the full energy $E_{\max} = [E_0 - q\phi(a)]$. The inward flux of ions at radius r' inside the cathode region is

$$\Gamma_i^{in}(r') = \frac{b^2}{r'^2} T_c h_i \Gamma_0 f_i(a) \exp[n_g \sigma_i^d(E_{\max})(r' - a)], \quad (62)$$

where the exponential term arises because of attenuation between a and r' and the grid transparency considers those lost on the grid. As these ions traverse the cathode region some of them undergo charge exchange to become fast neutrals. Using the same procedure as for the intergrid region, the number of neutrons produced in a shell of radius r and thickness dr due to inward traveling ions is

$$d^2\dot{N} = 8\pi b^2 n_g^2 \sigma_i^n(E_{\max}) \sigma_f\left(\frac{E_{\max}}{i}\right) T_c h_i \Gamma_0 f_i(a) \exp[n_g \sigma_i^d(E_{\max})(r' - a)] dr' dr. \quad (63)$$

Integrating over r gives

$$\int dr = \int_0^{r'} dr + \int_0^a dr + T_c \int_a^b dr + T_c T_a \int_b^c dr. \quad (64)$$

The first term is the contribution of the neutrals as they travel inward to the origin, the second is the contribution as they travel outward in the cathode region, the third is the contribution as they travel through the intergrid region, and the fourth is the contribution from the region between the anode and the vacuum wall. Evaluating the integral, we get

$$\int dr = r' + a + T_c(b - a) + T_c T_a(c - b) = C + r', \quad (65)$$

$$\text{where } C = a + T_c(b - a) + T_c T_a(c - b). \quad (66)$$

Consequently, the neutron production rate from inward traveling class I ions in the cathode region is

$$\dot{N} = 8\pi b^2 n_g^2 h_i \Gamma_0 f_i(a) T_c \sigma_i^n(E_{\max}) \sigma_f\left(\frac{E_{\max}}{i}\right) \int_0^a (r' + C) \exp[n_g \sigma_i^d(E_{\max})(r' - a)] dr'. \quad (67)$$

We also need to consider the fast neutrals, and their neutron production, generated by outgoing class I ions in the cathode region. The outgoing ion flux at r' is

$$\Gamma_i^{out}(r') = \frac{b^2}{r'^2} T_c h_i \Gamma_0 f_i(a) \exp[-n_g \sigma_i^d(E_{max})(r' + a)]. \quad (68)$$

Using the same arguments as above, the neutron generation rate from fast neutral-gas interactions resulting from these ions is

$$d^2 \dot{N} = 8\pi b^2 n_g^2 \sigma_i^n(E_{max}) \sigma_f \left(\frac{E_{max}}{i} \right) T_c h_i \Gamma_0 f_i(a) \exp[-n_g \sigma_i^d(E_{max})(r' + a)] dr' dr. \quad (69)$$

Integrating over r gives

$$\int dr = \int_r^a dr + T_c \int_a^b dr + T_c T_a \int_b^c dr = a - r' + T_c(b - a) + T_c T_a(c - b) = C - r', \quad (70)$$

so the neutron production rate becomes

$$\dot{N} = 8\pi b^2 n_g^2 \sigma_{in}(E_{max}) \sigma_f \left(\frac{E_{max}}{i} \right) T_c h_i \Gamma_0 f_i(a) \int_0^a \exp[-n_g \sigma_{id}(E_{max})(r' + a)] (C - r') dr'. \quad (71)$$

Adding the contributions from inward [Eq. (67)] and outward [Eq. (71)] traveling class I ions, and evaluating the integrals analytically gives

$$\dot{N} = 8\pi b^2 n_g \frac{\sigma_i^n(E_{max})}{\sigma_i^d(E_{max})} \sigma_f \left(\frac{E_{max}}{i} \right) T_c h_i \Gamma_0 f_i(a) \left[\left(a - \frac{1}{\alpha_i} + C \right) + \left(a + \frac{1}{\alpha_i} - C \right) e^{-2\alpha_i a} \right] \quad (72)$$

where $\alpha_i = n_g \sigma_i^d(E_{max})$.

The total neutron production from neutrals arising from class I ions of type i is the sum of the results in Eq. (61) and (72),

$$\begin{aligned} \dot{N}_{ni} = & 8\pi b^2 n_g^2 h_i \Gamma_0 \int_a^b \sigma_i^n(r') \sigma_f(r') \left\{ (r' + A) f_i(r') + T_c^2 (B - r') \left[\frac{f_i^{cp}}{f_i(r')} \right] \right\} dr' \\ & + 8\pi b^2 n_g \frac{\sigma_i^n \sigma_f}{\sigma_i^d} T_c h_i \Gamma_0 f_i(a) \left[\left(a - \frac{1}{\alpha_i} + C \right) + \left(a + \frac{1}{\alpha_i} - C \right) e^{-2\alpha_i a} \right], \quad i = 1, 2, 3. \end{aligned} \quad (73)$$

In the second line of Eq. (73) the cross sections are constants; σ_{in} and σ_{id} are evaluated at E_{max} and σ_f at E_{max}/i .

Equation (73) gives the neutron production due to neutrals generated from class I ions. These are a beam of ions (flux = $h_i \Gamma_0$) originating with very low energy at the anode ($r = b$) and traveling inward. We can use the same process to consider charge exchange neutrals coming from class II D^+ and D_2^+ ions; they are a beam (flux = $S_i(r'') dr''$) and originating with very low energy at the radius r'' . We make the substitutions

$$\begin{aligned} b^2 h_i \Gamma_0 & \rightarrow r''^2 S_i(r'') dr'', \\ E(r') & \rightarrow E(r', r''), \\ f_i(r') & \rightarrow \frac{g_i(r', r'')}{1 - T_c^2 g_i^{cp}(r'')}, \\ \frac{f_i^{cp}}{f_i(r')} & \rightarrow \frac{g_i^{cp}(r'')}{g_i(r', r'')} \left[\frac{1}{1 - T_c^2 g_i^{cp}(r'')} \right], \\ \int_a^b dr' & \rightarrow \int_a^{r''} dr', \end{aligned}$$

$$E_{\max} \rightarrow E(a, r'').$$

We make these replacements both for $i = 1$ (D^+) and $i = 2$ (D_2^+) and keep track of the energy of the fast nuclei produced when evaluating the fusion cross section. We also need to make one additional integration, namely over r'' .

For neutrons generated from neutrals arising from class II ions of type i ($i = 1$ for D^+ , $i = 2$ for D_2^+) we get

$$\begin{aligned} \dot{N}_{nli} = & 8\pi n_g^2 \int_a^b \int_a^{r'} \sigma_i^n [E(r', r'')] \sigma_f \left[\frac{E(r', r'')}{i} \right] \left\{ (r' + A) g_i(r', r'') + T_c^2 (B - r') \left[\frac{g_i^{cp}(r'')}{g_i(r', r'')} \right] \right\} dr' \frac{r''^2 S_i(r'')}{1 - T_c^2 g_i^{cp}(r'')} dr'' \\ & + 8\pi n_g T_c \int_a^b \frac{\sigma_i^n [E(a, r'')]}{\sigma_i^d [E(a, r'')] } g_i(a, r'') \sigma_f \left[\frac{E(a, r'')}{i} \right] \left[\left(a - \frac{1}{\alpha_i} + C \right) + \left(a + \frac{1}{\alpha_i} - C \right) e^{-2\alpha_i a} \right] \frac{r''^2 S_i(r'')}{1 - T_c^2 g_i^{cp}(r'')} dr'', \end{aligned} \quad (74)$$

$$\text{where } \alpha_i = n_g \sigma_i^d [E(a, r'')] \quad (75)$$

The total neutron production from fast neutral – background gas interactions is then

$$\dot{N}_n = \sum_{i=1}^3 \dot{N}_{nli} + \sum_{i=1}^2 \dot{N}_{nli}, \quad (76)$$

and the overall neutron production is the sum of the fast ion – background gas contribution [Eq. (43)] and the fast neutral – background gas contribution [Eq. (76)];

$$\dot{N} = \dot{N}_{ion} + \dot{N}_n. \quad (77)$$

C. Cathode current

A difficulty with our model so far is that we do not have a direct measurement of the ion flux, Γ_0 , crossing the anode and entering the intergrid region. However, the current to the cathode is normally measured experimentally. Consequently, we use the cathode current to determine Γ_0 . Within the context of our model, there are several contributions to the cathode current. The first is the contribution from class I D^+ , D_2^+ , and D_3^+ ions crossing the anode, heading inward, and being intercepted by the cathode grid. The second is the contribution from D^+ and D_2^+ ions born in the intergrid and cathode regions and intercepted by the cathode grid. These ions intercept the grid at finite energy and induce secondary electron emission; this also contributes to the measured cathode current. We allow for an energy- and species-dependent secondary electron emission coefficient, $\gamma_i(E)$. Cold ions produced in the cathode region ($r < a$), are contained by the electrostatic potential. They and the converging ion flow also produce a positive potential relative to the cathode grid that can trap electrons. If the cold ions reach the cathode grid before being neutralized by the electrons trapped in the cathode region, they are neutralized at the grid surface and contribute to the cathode current. However, if they are neutralized by the trapped electrons, then they don't contribute to the cathode current. The trapped electron physics is beyond the scope of this paper, so we consider both extremes to “bracket” the results.

The contribution from D^+ , D_2^+ , and D_3^+ ions being intercepted by the cathode grid is

$$I_i^1 = 4\pi q(1 - T_c) \Gamma_0 h_i b^2 \left[f_i(a) + T_c \frac{f_i^2(0)}{f_i(a)} \right] [1 + \gamma_i(qV_0)], \quad i = 1, 2, 3, \quad (78)$$

where $-V_0$ is the potential of the cathode. The first term in the square bracket in Eq. (78) is the contribution from ions hitting the outside of the cathode grid as they travel inward in radius, and

the second term is the contribution from ions hitting the inside of the cathode grid as they travel outward in radius. The factor T_c appears to the first power inside the square brackets since the outward traveling ions have traversed the cathode grid once to get to the cathode region.

The second part of the cathode current is that due to D^+ and D_2^+ ions being created at r and intercepting the cathode. This contribution is

$$I_i^2 = 4\pi q(1 - T_c) \int_a^b S_i(r) \left[g_i(a, r) + T_c \frac{g_{cpi}(r)}{g_i(a, r)} \right] \frac{r^2 \{1 + \gamma_i [E'(r)]\}}{1 - T_c^2 g_{cpi}(r)} dr, \quad i = 1, 2 \quad (79)$$

The terms in the square brackets in Eq. (79) represent the inward and outward traveling ions, respectively, hitting the cathode wires, just as for class I ions. The secondary electron emission coefficient is energy dependent and is therefore an implicit function of r through

$$E'(r) = q[\phi(r) - \phi(a)]. \quad (80)$$

Cold ions created by charge exchange and ionization at radii less than the cathode radius are trapped in an electrostatic well; they cannot penetrate to $r > a$, so they wander around and may eventually get collected by the cathode. Both class I and class II ions contribute to the source of these cold ions. The (non-directed) flux of class I ions of type i inside the cathode is

$$\Gamma_i(r) = \frac{b^2 h_i \Gamma_0}{r^2} T_c \left[f_i(r) + \frac{f_i^2(0)}{f_i(r)} \right], \quad (81)$$

where the attenuation function inside the cathode is

$$f_i(r) = f_i(a) \exp[-n_g \sigma_i^d (qV_0)(a - r)]. \quad (82)$$

Computing the rate of cold ion production by charge exchange and ionization and integrating over the cathode region, $r < a$, gives the number of cold ions produced per unit time by class I ions of type i within the cathode region; the current due to these ions is

$$I_i^3 = 4\pi q n_g \sigma_i^{tot} (qV) b^2 h_i \Gamma_0 T_c \int_0^a \left[f_i(r) + \frac{f_i^2(0)}{f_i(r)} \right] dr, \quad (83)$$

where

$$\sigma_i^{tot} = \sum_{j=1}^2 \sigma_{ij}^s, \quad (84)$$

all evaluated at the energy qV_0 . Because of the constant speed and the exponential variation of $f(r)$ inside the cathode, the above integral can be done analytically. The result is

$$I_i^3 = 4\pi q b^2 h_i \Gamma_0 T_c f_i(a) \frac{\sigma_i^{tot}(qV)}{\sigma_i^d(qV_0)} \left\{ 1 - \exp[-2n_g \sigma_i^d (qV_0)a] \right\}. \quad i = 1, 2, 3 \quad (85)$$

We neglect secondary electron emission induced by cold ions created within the cathode region since these ions hit the cathode at low energy.

The current due to cold ion production by charge exchange and ionization inside the cathode region by class II ions of type i is

$$I_i^4 = 4\pi q \int_0^a \int_a^b r'^2 n_g \sigma_i^{tot} [E(r, r')] S_i(r') T_c \left[g_i(r, r') + \frac{g_{cpi}(r')}{g_i(r, r')} \right] \frac{1}{1 - T_c^2 g_{cpi}(r')} dr' dr. \quad (86)$$

Inside the cathode the energy is constant, $E(r, r') = E(a, r')$, and the attenuation function $g_i(r, r')$ is given by

$$g_i(r, r') = g_i(a, r') \exp\{n_g \sigma_{id} [E(a, r)](r - a)\}. \quad (87)$$

Consequently, we can reverse the order of the two integrations in Eq. (86) and do the r -integration analytically. The result is

$$I_i^4 = 4\pi q T_c \int_a^b r'^2 \frac{\sigma_i^{tot} [E(r, r')]}{\sigma_i^d [E(a, r)]} \left[\frac{S_i(r') g_i(a, r')}{1 - T_c^2 g_{cpi}(r')} \right] \left(1 - \exp\{-2n_g \sigma_i^d [E(a, r)] a\} \right) dr' \quad (88)$$

The total cathode current is then

$$I_{cathode} = \sum_{i=1}^3 (I_i^1 + I_i^3) + \sum_{i=1}^2 (I_i^2 + I_i^4). \quad (89)$$

Equation (89) assumes the cold ions produced in the cathode region reach the cathode grid before being neutralized by trapped electrons. Alternatively, one can assume that the trapped electrons neutralize the cold ions before reaching the grid; in this case they do not contribute to the cathode current. The corresponding cathode current is then

$$I_{cathode} = \sum_{i=1}^3 I_i^1 + \sum_{i=1}^2 I_i^2 \quad (90)$$

Either Eq. (89) or (90) is used to determine the ion flux, Γ_0 , crossing the anode and heading towards the cathode. With this, the solution to the integral transport equations is fully determined, and we can calculate physical quantities of interest. In the next section, we consider both possibilities for cold ion contribution to the cathode current to bracket the predictions from this analysis.

D. Comparison with published experimental results

Spherical, gridded, inertial electrostatic confinement (IEC) devices are an important application of this analysis. The IEC concept was first patented by Farnsworth³ in the 1960s and advanced by Hirsch⁴ shortly thereafter. The IEC concept is of particular interest in the arena of non-power applications of fusion, such as neutron sources and high-energy proton sources for medical isotope production. The gridded IEC device has been extensively investigated by research groups around the world.⁵⁻¹¹ Neutron production rates measured in these devices provide experimental data for comparison with the predictions of our analysis. The Wisconsin IEC¹² device operating in the low-pressure regime (< 4 mTorr) fits the assumptions of our model the best, so we use it for comparison.

Shown in Fig. 3 is the comparison between the experimentally measured neutron production rate¹² and the rate predicted by the model. The experimental data is for a cathode diameter of 20 cm, anode diameter of 40 cm, background pressure of 2.5 mTorr, and a cathode current of 30 mA. The mix for the current into the intergrid region from the source region has been taken to be 71% D_3^+ , 23% D_2^+ , and 6% D^+ ions.¹³ If it is assumed that the cold ions in the cathode are neutralized by trapped electrons before reaching the cathode (curve I in Fig. 3), then the predicted neutron production rate is about 30% low compared with the experimental rate. But, if the cold ions in the cathode region are assumed to be neutralized at the cathode grid (curve II), then the calculated neutron production rate is a factor of four to five low, depending on the voltage. Note that, in both case I and case II, the slope of the neutron production with cathode voltage agrees well with the experimental results.

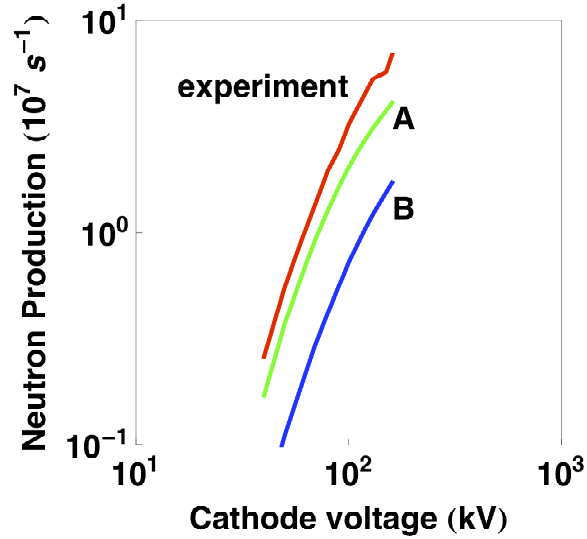


Figure 3. Comparison between experimental and calculated neutron production rates as a function of cathode voltage. A: model with cold ions in cathode region not included. B: model with cold ions in cathode region included.

It should be noted that the model does not consider fusion reactions arising from ion-ion collisions. Since the plasma is weakly ionized, this should be small. The model also does not include fusion reactions due to fast ions fusing with deuterium embedded in the near surface region of the grids and vacuum chamber. Experimentally, this has been measured¹⁴ to be small for D-D fusion under normal operating conditions, but can be significant for D-³He fusion.

Figure 4 shows the comparison of the measured¹² and calculated neutron production rates as a function of the background pressure while holding the cathode current constant at 60 mA; the experimental data is for a cathode diameter of 20 cm and anode diameter of 50 cm; the cathode voltage is constant at 100 kV. The pressure influences the results in several ways. First the target gas density increases with pressure. But attenuation of fast ions by charge exchange and dissociative processes also increase with pressure. This latter effect reduces the mean energy of the ions, which reduces the fusion rate. Finally, increasing pressure increases the formation of cold ions in the cathode region, which, for a given cathode current, has an effect on the ion flux crossing the anode and heading for the cathode. This latter effect is the reason for the greater sensitivity of case I in Fig. 4, compared with case II. A pressure effect not considered in our analysis is the ionization of gas by energetic electrons streaming from the cathode to the vacuum chamber wall.

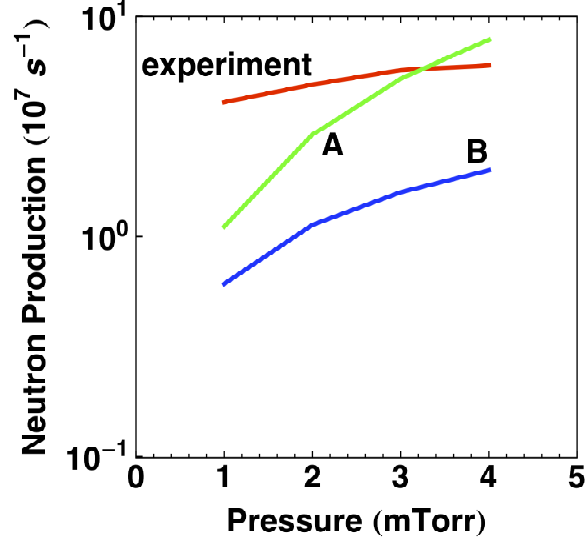


Figure 4. Comparison of experimental and calculated neutron production rates as a function of background pressure. A: model with cold ions in cathode region not included. B: model with cold ions in cathode region included.

In Fig. 4, the model shows more sensitivity to the background pressure than the measured values. One possible explanation for the different pressure sensitivity is that, while embedded fusion is small at normal operating pressure, it can become a larger fraction of the total fusion rate at lower pressure due to two effects. First, the reduced gas density reduces the target density and therefore the neutron production rate from fast ion and fast neutral fusion with the background gas. Second, the reduced gas density hardens the energy spectrum of the ions and neutrals impinging on the grids and walls, increasing the embedded fusion rate. Analyzing these effects to determine the embedded fusion contribution is beyond the scope of this paper.

V. SUMMARY AND CONCLUSIONS

A theoretical model for the effect of molecular interactions on the flow of molecular ions in spherically convergent geometry where the inner grid (cathode) is at a large negative potential and the outer grid (anode) is grounded has been developed. The model assumes a weakly ionized deuterium plasma composed of D^+ , D_2^+ , and D_3^+ ions which interact with the dominant background gas (D_2). The interactions included are charge exchange, ionization, and dissociative processes. The formalism developed includes the bouncing motion of the ions in the electrostatic well and sums over all generations of subsequent ions produced by atomic and molecular processes. This leads to a set of two coupled Volterra integral equations which are solved numerically. From the solution of the Volterra equations one can obtain quantities of interest, such as the energy spectra of the ions and fast neutral atoms and molecules, and the fusion reaction rate.

To provide an experimental test, the model is applied to inertial electrostatic devices and the calculated neutron production rate is compared with the measured value. The results show general agreement with the experimental results, but significant differences remain to be resolved. In particular, the model shows substantially more scaling with pressure than seen experimentally. The biggest uncertainty arises from not having a measurement of the ion current

across the anode. As a substitute, a relationship between the cathode current, which is measured experimentally, and the ion current has been developed. An uncertainty in this relationship is the extent to which electrons trapped in the center of the cathode region can neutralize cold ions formed there by charge exchange and ionization. If they do so, then the agreement between the model and experimental results is improved.

The formalism developed can be applied to other gases, depending on the availability of the relevant cross sections for molecular interactions.

ACKNOWLEDGMENTS

We gratefully acknowledge helpful discussions with the Wisconsin IEC experimental group, especially D. R. Donovan and D. R. Boris. This research is supported by the U.S. Department of Energy Grant No. De-FG02-04ER54745.

APPENDIX A: NUMERICAL SOLUTION OF TWO COUPLED VOLTERRA EQUATIONS

The method developed here is a modest extension of a standard method¹⁵ for solving single Volterra equations. We write the two coupled Volterra equations symbolically as

$$S^1 = A^1 + \int_r^b K^{11} S^1 dr' + \int_r^b K^{12} S^2 dr'$$

$$S^2 = A^2 + \int_r^b K^{21} S^1 dr' + \int_r^b K^{22} S^2 dr'$$

where we have switched from subscripts to superscripts to denote the species. We set up a uniform mesh (of width Δ and N points) with the subscript i denoting the mesh point. Using trapezoidal integration to evaluate the integrals, we get

$$S_i^1 = A_i^1 + \frac{\Delta}{2} K_{ii}^{11} S_i^1 + \Delta \sum_{j=i+1}^{N-1} K_{ij}^{11} S_j^1 + \frac{\Delta}{2} K_{iN}^{11} S_N^1 + \frac{\Delta}{2} K_{ii}^{12} S_i^2 + \Delta \sum_{j=i+1}^{N-1} K_{ij}^{12} S_j^2 + \frac{\Delta}{2} K_{iN}^{12} S_N^2$$

$$S_i^2 = A_i^2 + \frac{\Delta}{2} K_{ii}^{21} S_i^1 + \Delta \sum_{j=i+1}^{N-1} K_{ij}^{21} S_j^1 + \frac{\Delta}{2} K_{iN}^{21} S_N^1 + \frac{\Delta}{2} K_{ii}^{22} S_i^2 + \Delta \sum_{j=i+1}^{N-1} K_{ij}^{22} S_j^2 + \frac{\Delta}{2} K_{iN}^{22} S_N^2$$

We collect the i^{th} terms on the left and put the $j > i$ terms on the right.

$$S_i^1 \left(1 - \frac{\Delta}{2} K_{ii}^{11} \right) - \frac{\Delta}{2} K_{ii}^{12} S_i^2 = A_i^1 + \Delta \sum_{j=i+1}^{N-1} (K_{ij}^{11} S_j^1 + K_{ij}^{12} S_j^2) + \frac{\Delta}{2} (K_{iN}^{11} S_N^1 + K_{iN}^{12} S_N^2) \quad (\text{A1})$$

$$S_i^2 \left(1 - \frac{\Delta}{2} K_{ii}^{22} \right) - \frac{\Delta}{2} K_{ii}^{21} S_i^1 = A_i^2 + \Delta \sum_{j=i+1}^{N-1} (K_{ij}^{21} S_j^1 + K_{ij}^{22} S_j^2) + \frac{\Delta}{2} (K_{iN}^{21} S_N^1 + K_{iN}^{22} S_N^2) \quad (\text{A2})$$

We can view this as a set of two coupled equations (at any mesh point) in two unknowns, S_i^1 and S_i^2 . We write the 2 equations in matrix form,

$$\begin{pmatrix} 1 - \frac{\Delta}{2} K_{ii}^{11} & -\frac{\Delta}{2} K_{ii}^{12} \\ -\frac{\Delta}{2} K_{ii}^{21} & 1 - \frac{\Delta}{2} K_{ii}^{22} \end{pmatrix} \begin{pmatrix} S_i^1 \\ S_i^2 \end{pmatrix} = \begin{pmatrix} B_i^1 \\ B_i^2 \end{pmatrix}$$

where the B_i^1 and B_i^2 are the right hand sides of Eqs. (A1) and (A2). We use the inverse of the coefficient matrix to get a solution for the source functions S_i^1 and S_i^2 ,

$$\begin{pmatrix} S_i^1 \\ S_i^2 \end{pmatrix} = \frac{1}{\det} \begin{pmatrix} 1 - \frac{\Delta}{2} K_{ii}^{22} & \frac{\Delta}{2} K_{ii}^{12} \\ \frac{\Delta}{2} K_{ii}^{21} & 1 - \frac{\Delta}{2} K_{ii}^{11} \end{pmatrix} \begin{pmatrix} B_i^1 \\ B_i^2 \end{pmatrix} = \frac{1}{\det} \begin{pmatrix} \left(1 - \frac{\Delta}{2} K_{ii}^{22} \right) B_i^1 + \frac{\Delta}{2} K_{ii}^{12} B_i^2 \\ \frac{\Delta}{2} K_{ii}^{21} B_i^1 + \left(1 - \frac{\Delta}{2} K_{ii}^{11} \right) B_i^2 \end{pmatrix} \quad (\text{A3})$$

where the determinant of the coefficient matrix is

$$\det = \left(1 - \frac{\Delta}{2} K_{ii}^{11}\right) \left(1 - \frac{\Delta}{2} K_{ii}^{22}\right) - \frac{\Delta^2}{4} K_{ii}^{12} K_{ii}^{21} \quad (\text{A4})$$

We can solve Eq. (A3) at each point in the mesh by starting at the Nth mesh point, which is at the anode grid. From Eqs. (25) and (26)

$$S_N^1 = A_N^1 \quad (\text{A5})$$

$$S_N^2 = A_N^2 \quad (\text{A6})$$

since the integral terms do not contribute at this mesh point. Given the solution at the Nth mesh point, we get from Eq. (A3) the solution at the $i = N-1, N-2, N-3, \dots$ mesh points recursively. Hence a single sweep through the mesh determines the solution at all mesh points. This completes the solution of the coupled Volterra equations.

REFERENCES

- ¹G. A. Emmert and J. F. Santarius, *Atomic and molecular effects on spherically convergent ion flow I: single atomic species*, submitted to Physics of Plasmas.
- ²See National Technical Information Service Document No. DE91000527 (H.T. Hunter, M. I. Kirkpatrick, I. Alvarez, C. Cisneros, and R. A. Phaneuf, "Collisions of H, H₂, He, and Li atoms and ions with atoms and molecules," ORNL Report No. 6086, Vol. I, July 1990), pp. A-28, A-58, D-16, G-26, G-30, G-44 – G-54. Copies may be ordered from the National Technical Information Service, Springfield, VA 22161. The same cross section data is also available in the IAEA AMDIS database (<http://www-amdis.iaea.org/ALADDIN/>).
- ³P. T. Farnsworth, U.S. Patent No. 3,258,402 (28 June 1966).
- ⁴R. L. Hirsch, J. Appl. Phys. **38**, 4522 (1967).
- ⁵J. F. Santarius, G. L. Kulcinski, R. P. Ashley, D. R. Boris, B. B. Cipiti, S. K. Murali, G. R. Piefer, R. F. Radel, I. E. Radel, and A. L. Wehmeyer, Fusion Sci. Technol. **47**, 1238 (2005).
- ⁶G. H. Miley and J. Sved, Appl. Radiat. Isot. **48**, 1557 (1977).
- ⁷J. Park, R. A. Nebel, S. Stange, and S. Krupakar Murali, Phys. Rev. Lett. **95**, 015003 (2005).
- ⁸K. Yoshikawa, K. Masuda, T. Takamatsu, S. Shiroya, T. Misawa, E. Hotta, M. Ohnishi, K. Yamauchi, H. Osawa, and Y. Takahashi, Nucl. Instrum. Methods Phys. Res. B **261**, 299 (2007).
- ⁹H. Osawa, T. Kawame, S. Yoshioku, and M. Ohnishi, Proc. 20th IEEE/NPSS Symposium on Fusion Engineering, 2003 (IEEE, Piscataway, New Jersey, 2003), Vol. 3, p. 316.
- ¹⁰K. Yamauchi, M. Watanabe, A. Okino, T. Kohno, E. Hotta, and M. Yuura, Fusion Sci. Technol. **47**, 1229 (2005).
- ¹¹J. Khachan and S. Collis, Phys. Plasmas **8**, 1299 (2001).
- ¹²D. C. Donovan, D.R. Boris, G. L. Kulcinski, and J. F. Santarius, Fusion Sci. Technol. **56**, 507 (2009).
- ¹³D. R. Boris and G. A. Emmert, Phys. Plasmas **15**, 083502 (2008).
- ¹⁴S. Krupakar Murali, B. B. Cipiti, J. F. Santarius, and G. L. Kulcinski, Phys. Plasmas **13**, 053111 (2006).
- ¹⁵William H. Press, Brian R. Flannery, Saul A. Teukolsky, and William T. Vetterling, in *Numerical Recipes in Fortran: The Art of Scientific Computing* (Cambridge Univ. Press, New York, NY, 1992), p. 786.